

LARGE ORBIT GYROKLYSTRON DEVELOPMENT AT LOS ALAMOS

R. M. Stringfield, R. M. Wheat, D. J. Brown, M. V. Fazio, J. Kinross-Wright, B. E. Carlsten, G. Rodenz, R. J. Faehl, R. F. Hoerberling  
 Los Alamos National Laboratory, Los Alamos, New Mexico, 87545

Abstract

We have designed and are testing a large orbit gyroklystron amplifier for 1.3 GHz operation in 65 ns pulses. The ultimate power output goal is 500 MW with a gain in excess of 20 dB. This initial investigation is intended to lay the groundwork for operation at 11.4 GHz for particle accelerator applications, and also at frequencies of up to 35 GHz for other uses. Computational design has been performed with the resonant cavity code MAFIA and the particle in cell codes MERLIN and ISIS. Experimental measurements of the resonator modes were correlated with computational and analytical predictions. Electron beam optics through a magnetic cusp was also studied with ISIS and MERLIN, and verified experimentally, to develop a suitable electron beam trajectory from the diode into the resonator region. Performance tests of a single stage device have begun. The device is intended in its final form to use two resonators separated by an electron beam drift pipe.

Introduction

A large orbit gyrotron (gyroklystron) (LOG) amplifier operating at 1.3 GHz is being developed to operate at powers of up to 500 MW for 65 ns pulses. While this initial investigation is being performed at 1.3 GHz, this device can be scaled to higher frequencies in a straight forward fashion. LOG oscillators have operated at 15 GHz and higher frequencies with comparable performance to that at lower frequencies. Amplifier operation has been examined theoretically and experimentally, but less extensively [1-4].

These devices produce microwaves by the interaction of a helically rotating electron beam with the oscillating fields of a resonant cavity structure. The beam is formed by injecting a hollow, non-rotating beam, born in an axial magnetic field, through a magnetic cusp positioned at the anode plane. An annular slot is cut into the mild steel cusp plate to allow the beam to pass into the downstream resonator. In the cusp, a portion of the axial beam energy is converted to rotational energy. Typical ratios of rotational velocity to axial velocity (defined as alpha) are in the range of 1.5 to 2.5. The electron beam entering the resonator has an energy of 500-700 keV, a current of 1-3 kA, and a radius of 5-8 cm. The device, shown in Figure 1, employs a cylindrical resonator with three vanes in the wall spaced equally in azimuth.

The amplifier is designed as two resonator device, with cylindrical resonators of the type describe above. The vane structure is used to evoke coupling of the rotating electron beam with the TE(0,1,n) resonant cavity mode of the cylindrical structure by modifying the normally circular electric field pattern of the mode into a scalloped pattern, similar to the TE(3,1,n) mode, but near the lower TE(0,1,n) resonant frequency for a non-vaned cylindrical wall with an intermediate radius.

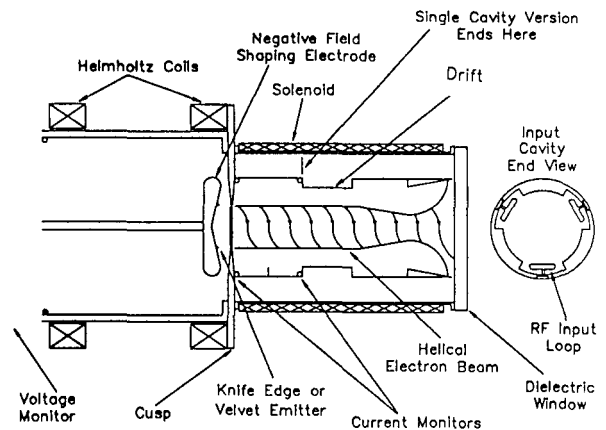


Figure 1. Large orbit gyrotron and gyroklystron geometry. Two resonator stages are shown, although single stage operation also will be investigated.

Rf is fed into the cavity using two loops, one in each of two of the vanes at the axial midplane. The standing wave pattern of the cavity will couple to the rotating beam, provided the beam angular velocity is in synchronism, in such a way that an azimuthal density perturbation will grow on the beam with three density maxima around the azimuth. The magnitude of the density variation will grow as the beam propagates down the length of the resonator, influenced both by the applied oscillating fields, and the space charge self fields of the beam that drive the negative mass instability. The instability will grow as the electron beam propagates through the system. Feedback from the beam instability drives the cavity fields to greater amplitude.

The downstream end of the first cavity has a central opening which forms the entrance to a cylindrical, non-vaned electron beam drift pipe. The pipe is intended to serve the role of an rf isolating sever between the first and second cavities, and also as a region in which the beam bunching can grow by the negative mass instability, independent of applied microwave fields. An optimum drift pipe length will be determined experimentally to maximize azimuthal beam bunching. A second, output resonator designed to be strongly coupled to the beam will be placed downstream of the drift pipe at the point of optimum beam bunching to extract rf energy. Mode converters suitable for transforming the TE01 circular waveguide mode of the output resonator into TE10 rectangular waveguide mode have been thoroughly studied since the 1950's. [5,6].

Computational Electron Beam Diode Studies

Particle-in-cell computer modelling was performed using the 2 dimensional versions of ISIS and MERLIN to design the electron gun and to optimize the electron beam trajectory.

Preliminary studies were performed with a computational technique known as synthesis. This technique steps the particles backward in position and time from the final state of the system (beam current, position, and velocity components), to determine the initial conditions (emission electrode position, shape, and potential) which lead to them, and a satisfactory trajectory through the device.

An acceptable synthetically generated diode configuration, shown in Figure 2, consists of a cathode emission annulus with a diameter of 14-14.2 cm, situated on a conical equi-potential surface at an angle of 67.5 degrees with respect to the symmetry axis. The distance between the emission annulus and the anode was 2.2 cm, yielding an cathode electric field of 300 kV/cm at a voltage of 650 kV. The annular opening at the anode through which the beam passes into the resonator drift section has a mean diameter of 12.5 cm and is 1 cm wide.

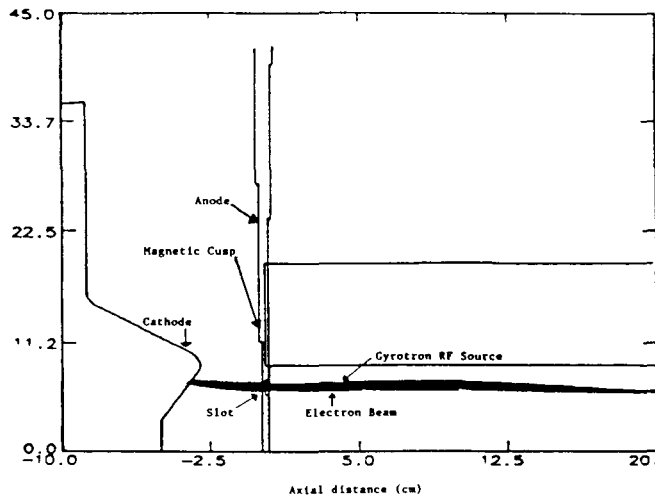


Figure 2. Particle-in-cell computer model of the baseline design of a suitable electron beam diode and transport geometry.

The synthetic computation was the starting point for conventional calculations of beam dynamics moving forward in time. A conventional run using the diode and drift pipe parameters found from the synthetic calculations agreed with the synthetic calculation prediction. All of the current emitted from the cathode, up to a maximum of 2.7 kA, passed through the cusp and drifted with little radial oscillation in the resonator region.

### Experimental Diode Results

Diode hardware was built with the guidance of the computer modelling. The experimental diode geometry is shown in Figure 1. Emission was evoked from an annular region of the angled surface either by mounting a knife edged ring or a belt of velvet on the surface as an explosive emission emitter. The diameter of the emitting ring was varied from 11.4 to 14 cm. The drift pipe had no vane structure for these diode experiments, to simulate the conditions of the computer model.

Alpha, the ratio of rotational velocity to axial velocity of the electron beam, was measured using a quartz witness plate interposed in the beam path. A pattern of the electron deposition at the plate location can be seen in luminosity of the quartz. By

attaching a metal rectangle upright on the upstream side of the quartz at the radius of the beam, a shadow is cast on the quartz by the metal obstruction. The ratio of the length of the shadow to the height of the obstruction is a determination of alpha.

Alpha was measured to be in the range of 1.5 to 2.0 for a magnetic field of 400 gauss, and in the range of 2.0 to 2.5 with a magnetic field strength of 500 gauss. This set of conditions most closely matched those found by the computer modelling to provide good beam transport.

Using a knife edge emitter with a diameter of 12.4 cm, a magnetic field of 300 to 400 gauss, and a diode voltage of 700 kV, 3 kA was transported past the cusp with an alpha of 1.5. Waveforms for this case are shown in Figure 3. These lower magnetic field conditions are those anticipated for the 1.3 GHz amplifier experiments. The computer study did not include these parameters in its investigation, but rather had used values of magnetic field of 500 gauss at the cathode, based upon the needs of an amplifier designed for higher frequency.

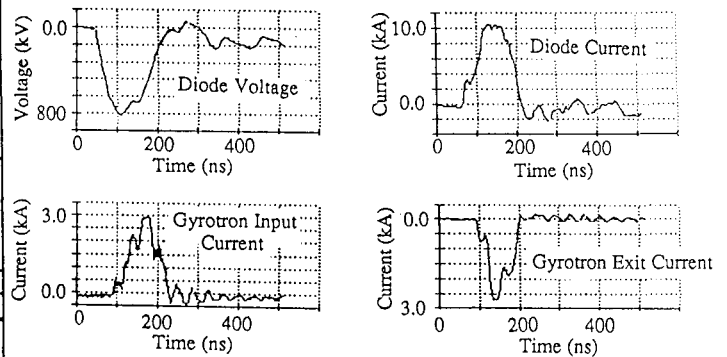


Figure 3. Waveforms for the diode voltage, diode current, current immediately downstream of the cusp, and 30 cm downstream. The magnetic field at the cathode was 330 gauss.

### Studies of the Resonant Cavity Modes

An extensive study of the cavity modes of the resonant structure for this device has been performed using the electromagnetic field solving code MAFIA, analytic modelling, and cold test measurements of structures performed with a vector network analyzer. Figure 4 shows the frequencies measured with a network analyzer connected to magnetic loop probes in the cavity, oriented to couple to the TE(0,1,n) modes. The peak of interest, the TE(0,1,0.5) mode, oscillates at 1,280 Hz. Figure 5 shows the MAFIA calculated electric field pattern for this mode at 1277 MHz, showing good agreement with the cold test measurement. Testing the input cavity with the downstream end fully open, the cavity has a Q of 45. As a two stage device, the first stage Q will be much higher, of the order of several hundred, but has not been established. The output cavity Q of the two stage device will be similar to that of the single stage resonator, in the range of 25 to 100.

### Experimental Studies

The experimental configuration consists of the diode, cusp

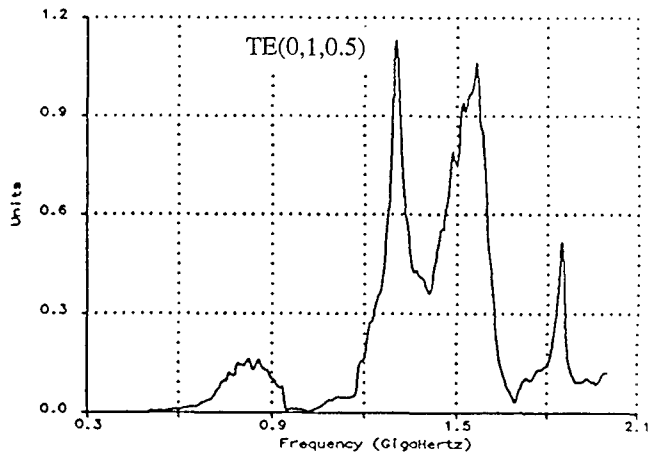


Figure 4. Linear plot of relative signal amplitude vs frequency in the resonant cavity of the single stage device. One cylinder end is open. Strong resonance is seen at the desired frequency of 1280 MHz.

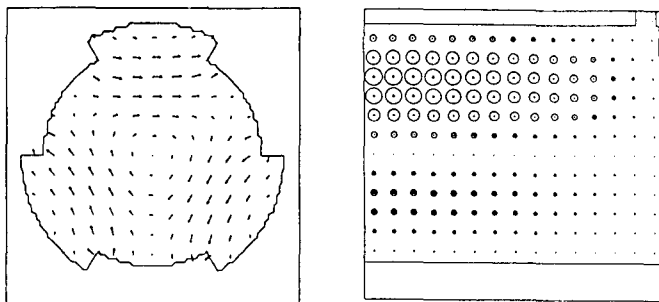


Figure 5. MAFIA electric field map for the single open ended resonator resonating at 1277 MHz.

and magnetic field coils, downstream resonator section, and a dielectric vacuum window for radiating the microwaves into an anechoic volume downstream of the vacuum chamber. A 4 kW 1.3 GHz source provides rf input drive to the resonator in these initial studies. Up to 20 MW is available as input drive but will require device modifications for aperture coupling to accommodate the power. Presently, magnetic loops are situated at the base of two of the vanes for cavity input drive. A loop in the third vane is used to monitor the standing wave field in the cavity. A stub waveguide receiver is positioned in the anechoic volume downstream of the open resonator end to monitor the radiated power in the far field.

We evaluate amplifier performance by comparing the radiated microwave power in three different circumstances. First, the radiated power due to the 4 kW input drive alone is measured. Second, the radiated power with no input drive, but with the electron beam injected, is measured. Finally, the radiated power when both input rf drive and injected electron beam are present in the resonator is measured. Relative power measurements among shots are performed by comparing

detected signals received with a waveguide stub placed at a fixed location in the far field downstream of the open ended resonator.

With no input drive, the radiated rf power pulse was narrow in time, 42 ns long, with a wide statistical standard deviation of 24 ns, or 56 percent. This duration is significantly less than the FWHM duration of the electron beam current in the resonator, approximately 65 ns. In addition the mean value of the peak power, while larger than with input drive, had a 28 percent standard deviation. With input drive the output power pulse continued for 60 ns, nearly the length of the electron beam, with a standard deviation of 16 ns, or 27 percent. The peak power of the output pulse using input drive was 26 percent lower than without input drive, but was longer by 50 percent with a smaller standard deviation of 16 ns, or 27 percent. The FWHM of the fast Fourier transform of the rf signal was 36 MHz (25 MHz standard deviation) without input drive, and 27 MHz (17 MHz standard deviation) with input drive. Hence, there was clear improvement in the output power pulse associated with the application of input rf drive, in total energy of the output pulse, the frequency purity, and in reducing the statistical scatter between pulses.

### Summary

The study and construction of a large orbit gyrotron and two stage gyrokystron amplifier are underway. Modelling and experiments have been performed to design these devices. Experiments are ongoing to measure and optimize the performance of the single stage device, in preparation for subsequent two stage operation. Improvements in the quality of the rf output pulse produce by the first (rf input) cavity of the device have been found as the result of injecting input rf power into the cavity. This work has been supported by the Los Alamos National Laboratory Independent Research and Development Program, sponsored by the U. S. Department of Energy.

1. W. W. Destler, et al, "High-power microwave generation from large-orbit devices," IEEE Trans. on Plasma Science PS-16 (2), April 1988, p71.
2. Y. Y. Lau and L. R. Barnett, "Theory of a low magnetic field gyrotron (gyromagnetron)," Int. J. of Infrared and Millimeter Waves 3 (5), 1982, p. 619.
3. J. Y. Choe, K. Boulais, V. Ayres, W. Namkung, and H. Uhm, "Preliminary study of cusptron amplifier," Microwave and Particle Beam Sources and Directed Energy Concepts, SPIE 1061 (1989) p. 132.
4. K. R. Chu, et al, "Theory, design, and operation of large-orbit high harmonic gyrokystron amplifiers," IEEE Trans. on Plasma Science PS-13 (6), December 1985, p 435.
5. S. S. Saad, et al, "Analysis and design of a circular TE01 Mode Transducer," Microwaves, Optics, and Acoustics 1 (2), p. 58.
6. S. E. Miller, "Coupled wave theory and waveguide applications," Bell System Journal, May 1954, p. 661.